ACS Chemical Neuroscience

Research Article

pubs.acs.org/chemneuro

Role of the ρ1 $GABA_C$ Receptor N-Terminus in Assembly, Trafficking and Function

Lik-Wei Wong,[†,‡] Han-Shen Tae,[†] and Brett A. Cromer*[,†]

[†]Health Innovation Research Institute, School of Medical Sciences, RMIT University, Bundoora, Victoria 3083, Australia

[‡]Department of Pharmacology and Therapeutics, University of Melbourne, Parkville, Victoria 3010, Australia

Supporting Information

ABSTRACT: The $GABA_C$ receptor and closely related $GABA_A$ receptor are members of the pentameric ligand-gated ion channels (pLGICs) superfamily and mediate inhibitory fast synaptic transmission in the nervous system. Each pLGIC subunit comprises an N-terminal extracellular agonist-binding domain followed by a channel domain and a variable intracellular domain. Available structural information shows that the core of the agonist-binding domain is a β sandwich of ten β-strands, which form the agonist-binding pocket at the subunit interface. This β-sandwich is preceded by an N-terminal α-helix in eukaryotic structures but not in prokaryotic structures. The N-terminal α-helix has been shown to be functionally essential in α7 nicotinic acetylcholine receptors. Sequence analysis of $GABA_C$ and $GABA_A$ receptors predicts an α-helix in a similar position but preceded by 8 to 46 additional residues, of unknown function, which we term the N-terminal extension. To test the functional role of both the N-terminal extension and the putative N-terminal α-helix in the ρ1 $GABA_C$ receptor, we created a series of deletions from the N-terminus. The N-terminal extension was not functionally essential, but its removal did reduce both cell surface expression and cooperativity of agonist-gated channel function. Further deletion of the putative N-terminal α-helix abolished receptor function by preventing cell-surface expression. Our results further demonstrate the essential role of the N-terminal α-helix in the assembly and trafficking of eukaryotic pLGICs. They also provide evidence that the N-terminal extension, although not essential, contributes to receptor assembly, trafficking and conformational changes associated with ligand gating.

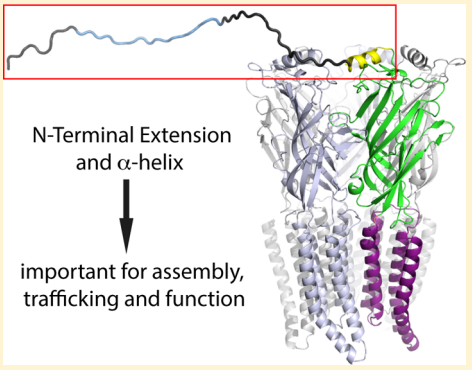

KEYWORDS: *Ion channel, $GABA_C$ receptor, ligand-gating, protein trafficking, microfluidic electrophysiology*

Pentameric ligand-gated ion channels (pLGICs), also known as Cys-loop LGICs due to a conserved disulfide bond, are transmembrane ion channels that are opened by the binding of an agonist to an N-terminal extracellular domain. The pLGIC superfamily includes both cation-selective channels that mediate excitatory neurotransmission, such as the nicotinic acetylcholine receptor (nAChR) and serotonin receptor ($5HT_3R$), and anion-selective channels that primarily mediate inhibitory neurotransmission, such as the glycine receptor (GlyR) and γ-aminobutyric acid type A/C receptor ($GABA_{A/C}R$).[1] The $GABA_CR$ was originally identified as pharmacologically distinct from bicuculline-sensitive $GABA_AR$ LGICs and baclofen-sensitive $GABA_B$ G-protein coupled receptors.[2] Based on primary sequence and function, however, $GABA_A$ and $GABA_C$ are clearly closely related pLGIC superfamily members and distinct from $GABA_BR$. To date, three human $GABA_CR$ subunits (ρ1, ρ2, and ρ3) have been identified.[3−5] Unlike $GABA_ARs$, ρ subunits can form functional homomeric $GABA_CRs$ but different ρ subunits can also coassemble to form heteromeric receptors.[6,7] There is also evidence that ρ subunits can form functional heteromeric receptors with $GABA_AR$ subunits.[8−13]

The structure of pLGICs has been extensively studied for the past 30 years, with our knowledge of their structure at atomic resolution advancing dramatically in the past decade. The first high resolution crystal structure of a pLGIC-related protein was solved by Brejc and colleagues,[14] revealing the structure of an acetylcholine-binding protein (AChBP) from the snail *Lymnaea stagnalis*. It is a soluble homopentamer, homologous to the extracellular domain of nAChR without an attached transmembrane domain. The first structure of a full length pLGIC at a resolution sufficient to build an atomic model was resolved from the cryo-electron microscopy of *Torpedo* nAChR at 4 Å resolution[15,16] and more recently in both open and closed states.[17] These structures have shed light on the architecture and structure of pLGICs and hence have been widely used as templates for homology modeling.[18−20] Several prokaryotic homologues of pLGICs have been identified,[21] and high-resolution structures have been determined for two of these from *Erwinia chrysanthemi* (ELIC) and *Gloeobacter violaceus* (GLIC).[22−25] Recently, Hibbs and Gouaux[26] resolved the

Received: December 9, 2013
Accepted: October 9, 2014
Published: October 27, 2014

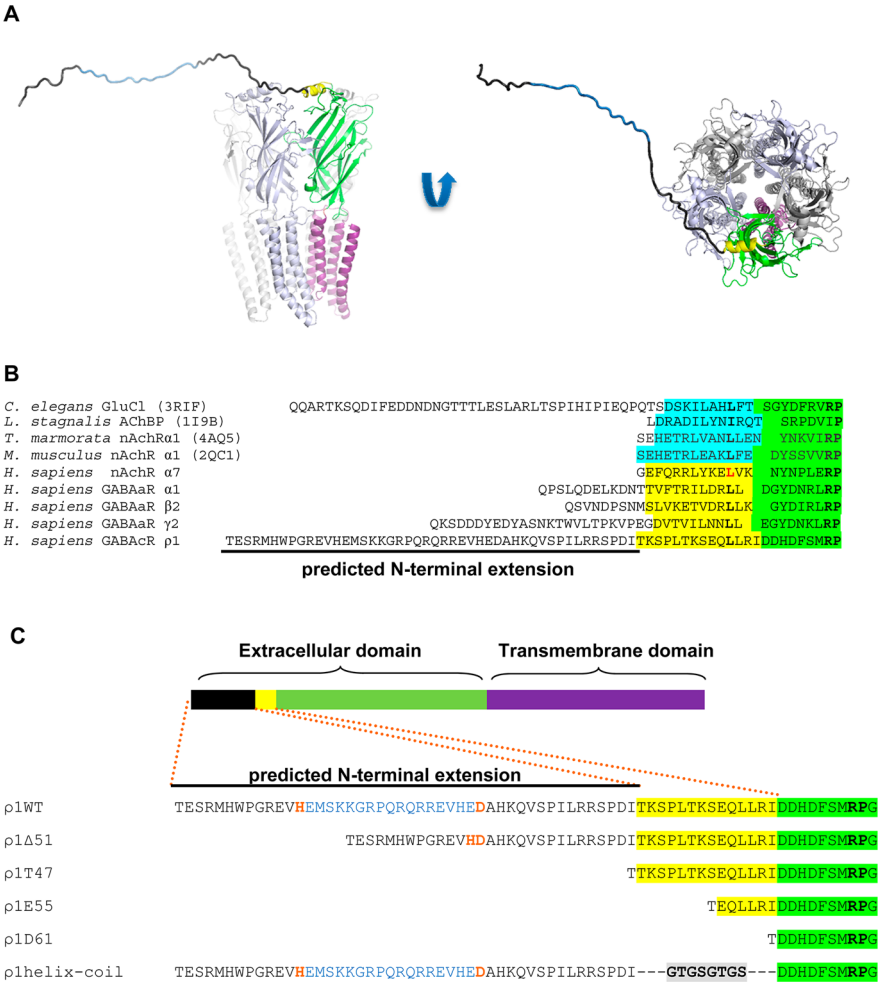

Figure 1. Molecular model and sequence alignment of pLGICs. (A) Comparative model of human ρ1 $GABA_CR$ built by homology to GluCl structure 3RIF,[26] shown in ribbon representation viewed along the symmetry axis from the extracellular side (left) and orthogonal to the symmetry axis (right), extracellular domain above membrane domain. One subunit is shown with the N-terminal extension as random coil (black), including Δ51 residues (blue), putative N-terminal α-helix (yellow), β-sandwich domain (green), and membrane domain (purple). This coloring maintained in panels B and C. Remaining subunits colored gray or pale blue. (B) pLGIC N-terminal amino acid sequence alignment (excluding signal peptides) of N-terminal α-helices from crystal structures (cyan), with PDB code given, and Jpred3 α-helix predictions (yellow). A ClustalW alignment was manually adjusted for structural alignment and to align a partly conserved dileucine motif, including α7 nAChR L11 (red text). Highly conserved residues are shown in bold. (C) Schematic representation of ρ1 $GABA_CR$ subunit and amino acid sequence of the N-terminal region showing the N-terminal extension, a generous definition of putative N-terminal α-helix, and the region absent in splice variant Δ51 (blue text), followed by each of the deletion constructs. The putative helix is replaced with an eight residue predicted random coil (bold) in the "helix–coil" mutant.

structure of the invertebrate *Caenorhabditis elegans* glutamate-gated chloride channel (GluCl), the first structure of a chloride-selective pLGIC and a good template for modeling of GlyRs and $GABA_A/_CRs$. Very recently, the first high-resolution structures of mammalian pLGICs have been determined, a homopentameric human β3 $GABA_AR$[27] and a mouse $5HT_{3A}R$,[28] both of which are consistent with the overall architecture of earlier structures.

All resolved structures share a similar overall fold, consisting of five identical or similar subunits surrounding the central pore in the membrane (Figure 1A). Each subunit can be functionally separated into three domains: a large N-terminal extracellular domain, followed by four transmembrane (TM) α-helices forming the channel domain and a variable intracellular domain between TM3 and TM4. The agonist-binding site is formed by several loops and β-strands at the intersubunit interface of the extracellular domain. In eukaryotic structures, the core β-sandwich is preceded by an N-terminal α-helix that sits on top of the β-sandwich of each subunit (Figure 1A). The N-terminus of this helix is close to the adjacent subunit but makes relatively minor contact across the intersubunit interface in either nAChR[17] or GluCl structures.[26] Although sequence conservation is poor in this region, secondary structure prediction algorithms consistently predict an α-helix in a similar position for other eukaryotic pLGIC subunits (Figure 1B).[18] Somewhat surprisingly, however, an N-terminal α-helix is not present in the structures of either prokaryotic pLGIC, ELIC or GLIC. Despite this absence, these prokaryotic pLGICs are functional. Although the binding site of agonistic protons is not clearly defined for GLIC, ELIC is clearly activated by ligands at the canonical agonist-binding site.[29] The absence of an N-terminal α-helix in functional prokaryotic pLGICs raises the question of whether one is essential for the structure or function of eukaryotic pLGICs.

This question has been addressed by Castillo et al.,[30] who demonstrated that deletion or mutation of the putative N-

dx.doi.org/10.1021/cn500220t | *ACS Chem. Neurosci.* 2014, 5, 1266–1277

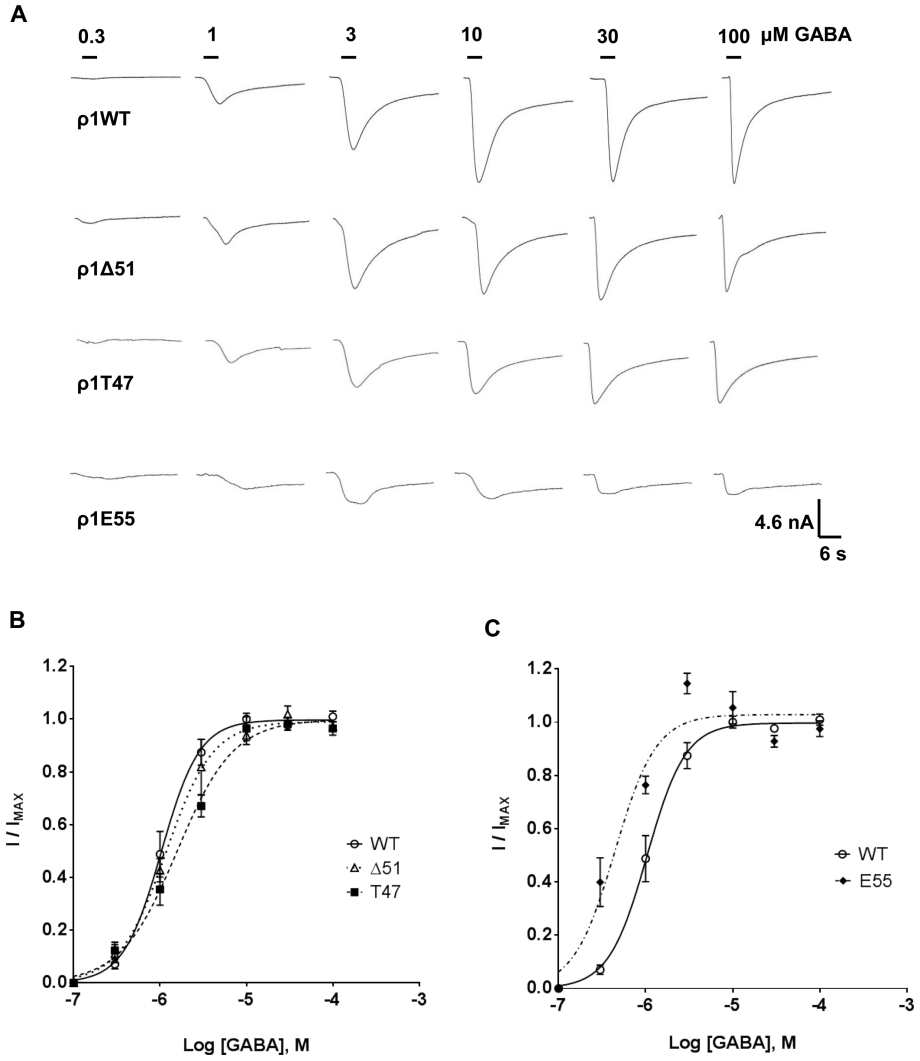

Figure 2. Whole-cell current traces and GABA dose–response curves. (A) Representative whole-cell currents from HEK-293T cells expressing ρ1WT, ρ1Δ51, ρ1T47, and ρ1E55. The indicated concentrations of GABA (μM) were applied for 3 s to cells voltage-clamped at −80 mV. (B) Normalized GABA dose–response curves for cells expressing WT, Δ51, and T47 ρ1 $GABA_CR$ and (C) WT and E55 ρ1 $GABA_CR$, with curves fitted to the Hill Equation. Error bars represent SEM, n = 4–7.

terminal α-helix of α7 nAChRs prevented receptors from reaching the cell surface of *Xenopus* oocytes, as detected by fluorescent α-bungarotoxin binding, and hence abolished receptor function. Another study by Bar-Lev et al.,[31] which investigated chimeric α7 nAChR–GluCl receptors expressed in cultured mammalian cells, also showed that deletion of the N-terminal α-helix abolished fluorescent α-bungarotoxin-binding sites at the cell surface. In this second study, cell surface receptors were detected, however, using alternative labeling of N-terminally HA-tagged subunits with an anti-HA antibody.[31] This data indicates that some nonfunctional α7 nAChR–GluCl protein did reach the cell surface but the amount of mutant receptor at the cell surface, relative to WT, was not quantified. Despite the differences in these studies, both show that removal of the N-terminal α-helix eliminates functional α7 nAChRs at the cell surface.

Mature nAChR subunits only have one or two residues prior to the N-terminal α-helix, but other pLGICs, particularly anion-selective GlyR, $GABA_AR$, and $GABA_CR$, have significant additional residues prior to the putative N-terminal α-helix (Figure 1B). We call these extra residues the "N-terminal extension". Its position at the N-terminus of the putative α-helix places the N-terminal extension in close apposition to the neighboring subunit where it could contribute to intersubunit interactions (Figure 1A). The N-terminal extension in ρ1 $GABA_CR$ is predicted to be 46 residues, much larger than most other N-terminal extensions. Despite the demonstrated significance of the N-terminal α-helix in α7 nAChRs[30,31] described above, its role remains unclear in other pLGICs. This uncertainty prompted us to investigate the role of both the putative N-terminal α-helix and the N-terminal extension in ρ1 $GABA_CR$ assembly, trafficking and function.

RESULTS

An automated microfluidic electrophysiology platform (IonFlux-16 System) was used to measure total whole-cell GABA-activated currents from a population of up to 20 cells, similar to work of Chen et al.[32] Typical currents in response to a 3 s application of GABA are shown in Figure 2A. The GABA concentration required to elicit half-maximum response (GABA EC_{50}) for ρ1WT was 1.0 ± 0.1 μM with a Hill coefficient of 2.3

dx.doi.org/10.1021/cn500220t | ACS Chem. Neurosci. 2014, 5, 1266–1277

± 0.2 as shown in Table 1, similar to previous reports for human ρ1 $GABA_CR$ EC_{50} expressed in HEK-293 cells.[6,33]

Functional Effects of Deletions to the N-Terminal Extension. To determine the functional role of the N-terminal extension, we created deletion constructs shown in Figure 1C, ρ1T47 lacking the N-terminal extension (residues 2−46) and ρ1Δ51 lacking a section of the N-terminal extension coded by exon 2 (residues 14−30), which recapitulates a previously described alternate spliced form of ρ1 $GABA_CR$ identified in human retina.[2,34] Both ρ1Δ51 and ρ1T47 deletions showed robust GABA-activated currents that were broadly similar to ρ1WT (Figure 2). The GABA EC_{50} (1.3 ± 0.1 μM) for ρ1T47 was not significantly different compared with ρ1WT ($p > 0.05$) but the Hill coefficient (1.4 ± 0.2) was significantly reduced ($p < 0.05$) (Table 1). For ρ1Δ51, neither the GABA EC_{50} (1.2 ± 0.1 μM) nor the Hill coefficient (1.7 ± 0.3 (Table 1)) were significantly different from WT. These results differed slightly from a previous study that used *Xenopus* oocytes to express ρ1WT and ρ1Δ51 and found that the ρ1Δ51 deletion caused a 2-fold decrease in GABA EC_{50}.[2] This difference may be due to the different expression systems used, which do show differences in the kinetics of ρ1 $GABA_CR$ GABA-activated currents.[33] The population whole-cell peak current (I_{max}) for ρ1T47 (7.4 ± 0.4 nA) was significantly reduced ($p < 0.01$) compared with ρ1WT (13.1 ± 1.0 nA) (Figure 3). There was also a significant 33% decrease ($p < 0.05$) in the peak current for ρ1Δ51 (8.8 ± 1.0 nA) relative to ρ1WT.

Table 1. GABA Dose-Response Parameters for ρ1 $GABA_CR$ WT and Deletion Constructs[a]

construct	GABA EC_{50} (μM)	Hill coefficient (n_H)	maximum current, I_{max} (nA)	n
WT	1.0 ± 0.1	2.3 ± 0.2	13.1 ± 1.0	6
Δ51	1.2 ± 0.1	1.7 ± 0.3	8.8 ± 1.0*	5
T47	1.3 ± 0.1	1.4 ± 0.2*	7.4 ± 0.4**	7
E55	0.4 ± 0.1	2.5 ± 0.5	3.4 ± 0.3****	4
D61				3
helix−coil			1.0 ± 0.1****	4

[a]Values are means ± SEM. Asterisks indicate significant differences: *$p < 0.05$, **$p < 0.01$, and ****$p < 0.0001$ compared with ρ1WT.

We next sought to determine whether decreases in whole-cell peak current were due to reduced total subunit expression or reduced receptor trafficking to the cell surface. Cell surface and total expression of ρ1WT and mutants were detected by indirect immuno-fluorescent labeling of intact and permeabilized cells, respectively, with an N-19 anti-ρ1 antibody that recognizes a peptide in the extracellular N-terminal domain. Fluorescent labeling per cell was quantified by flow cytometry, and the mean fluorescence for each mutant was compared with WT, measured in the same experiment, after subtracting background fluorescence from untransfected cells. Cells transfected with an unrelated protein showed background fluorescence that was indistinguishable from untransfected cells (data not shown).

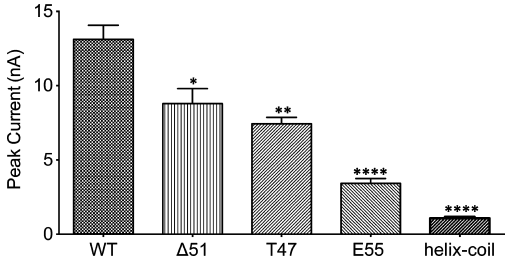

Figure 3. Effect of ρ1 $GABA_CR$ N-terminal deletions on peak currents (nA). Population whole cell peak currents are shown for ρ1WT and mutants Δ51, T47, E55, and helix−coil. Data represent means ± SEM, $n = 4–7$. Asterisks indicate significant differences: *$p < 0.05$, **$p < 0.01$, and ****$p < 0.0001$ compared with ρ1WT.

The N-19 immunofluoresence histogram for nonpermeabilized cells transfected with ρ1WT showed a broad peak above background fluorescence from untransfected cells (Figure 4A). A similar broad peak was seen for permeabilized cells but with the peak maximum shifted toward higher fluorescence. In general each fluorescence histogram of transfected cells did not show clearly separable peaks corresponding to transfected and untransfected cells indicating that the percentage transfected was high but with a wide range in expression levels. Consequently, we did not use a gate to remove untransfected cells from our analysis and determined the mean fluorescence for the whole population of cells. For ρ1Δ51, there was no significant difference in the mean total receptor expression relative to ρ1WT (Figure 4C; 101% ± 10% of ρ1WT, $p > 0.05$) but there was a significant decrease in receptor detected at the cell surface at 76% ± 7% of ρ1WT ($p < 0.05$).

Conversely, we failed to detect either surface or total expression of ρ1T47 with the N19 antibody. Because these findings were inconsistent with robust GABA-activated currents for ρ1T47 shown above, we suspected that the N-19 epitope had been removed with deletion of residues 2−46 in ρ1T47. Although we do not know the exact epitope recognized by the N-19 antibody, because it is considered proprietary information (Santa Cruz Biotechnology), we do know it is within the region including residues 10−60 of human ρ1. Western blotting with the N-19 antibody reliably detected ρ1WT but not ρ1T47 (data not shown), supporting the removal of the N-19 epitope in ρ1T47. Interestingly, we were also unable to detect ρ1Δ51 with the N-19 antibody by Western blot (data not shown), although it was detected by flow cytometry (Figure 4).

To provide an alternative to antibodies against the ρ1 N-terminal region, which may bind in the segments we have deleted, all ρ1 $GABA_CR$ constructs were C-terminally His-tagged. A mouse anti-His tag antibody was then used to assess both surface and total expression of ρ1T47 (Figure 5). The ρ1T47 mutant showed a significant reduction in receptors at the cell surface (49.7% ± 5.7% of ρ1WT, $p < 0.05$), but the total expression was similar to ρ1WT (94.5% ± 8.2% of ρ1WT, $p > 0.05$, Figure 5). The decrease in surface expression was consistent with the reduction in whole-cell peak current in ρ1T47.

Functional Effects of Further Deletions into the Putative N-Terminal α-Helix. To determine the functional role of the putative N-terminal α-helix, we created further deletion constructs (Figure 1C), ρ1E55 lacking the N-terminal extension and half of the putative α-helix (residues 2−54), and ρ1D61, lacking the N-terminal extension and all of the putative α-helix (residues 2−60). The ρ1E55 construct produced a functional receptor that showed dose-dependent GABA-activated currents (Figure 2). The current amplitudes were, however, small and inconsistent and showed marked rundown of currents in response to repeated applications of GABA, particularly at higher GABA concentrations. Consequently, the GABA EC_{50} for ρ1E55 was difficult to measure reliably, and

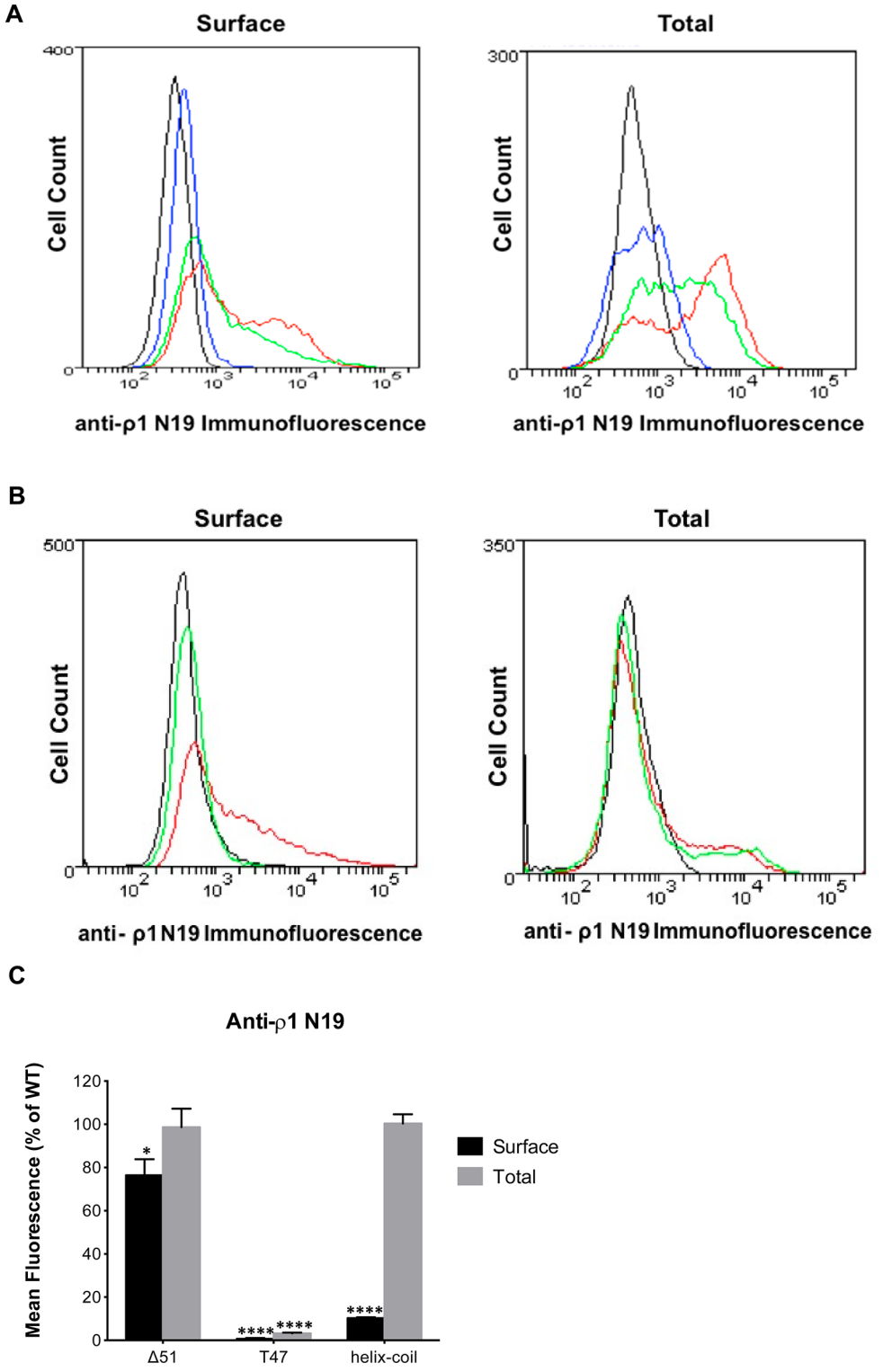

Figure 4. Anti-ρ1 (N19) immunodetection of cell surface and total expression of ρ1Δ51 and ρ1T47 and helix−coil relative to ρ1WT. (A) Immunofluorescence intensity histograms of cell surface staining of intact HEK-293T cells (left) or total staining of permeabilized cells (right) that were either untransfected (black) or transfected with ρ1WT (red), ρ1Δ51 (green) or ρ1T47 (blue). (B) Immuno-fluorescence intensity histograms of cell surface staining of intact HEK-293T cells (left) or total staining of permeabilized cells (right) that were either untransfected (black) or transfected with ρ1WT (red) or helix−coil (green). (C) Average population mean fluorescence relative to WT (as %) from four to five separate experiments. Error bars indicate ± SEM; *p < 0.05 and ****p < 0.0001 compared with ρ1WT.

while it apparently is lower than for that WT, we do not consider this a significant change. The population whole-cell peak current (I_{max}) for ρ1E55 (3.4 ± 0.3 nA) was significantly reduced to 25% (p < 0.0001) of ρ1WT currents. This was consistent with significantly lower levels of ρ1E55 at the cell surface, showing only 28.0% ± 1.7% of ρ1WT (p < 0.0001). Reduced surface expression was not due to a decrease in total

dx.doi.org/10.1021/cn500220t | ACS Chem. Neurosci. 2014, 5, 1266−1277

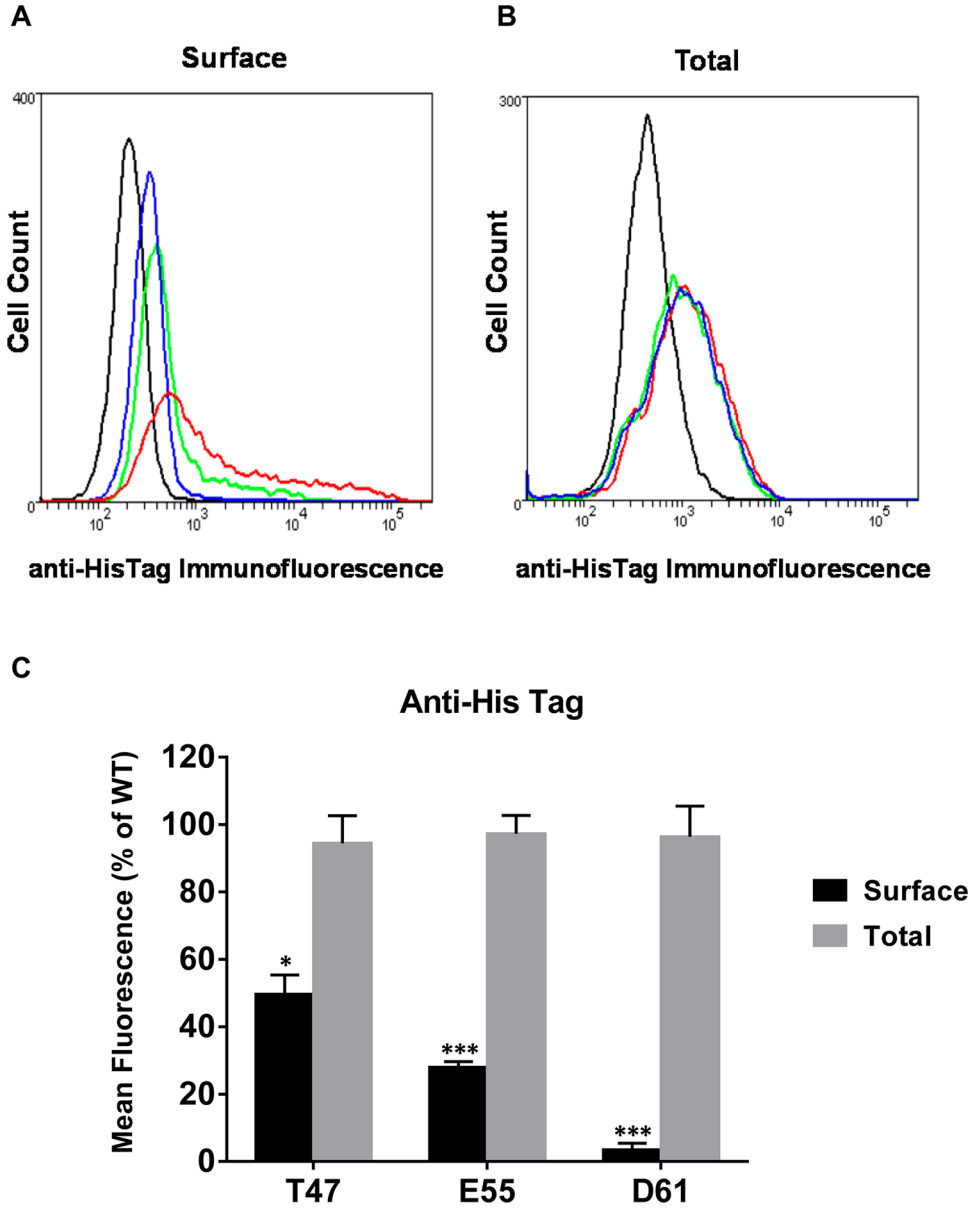

Figure 5. Anti-His Tag immunodetection of cell surface and total expression of ρ1T47, ρ1E55, and ρ1D61, relative to ρ1WT. Immunofluorescence intensity histograms of (A) cell surface staining of intact HEK-293T cells or (B) total staining of permeabilized cells that were either untransfected (black) or transfected with ρ1WT (red), ρ1T47 (green), or ρ1D61 (blue). (C) Average population mean fluorescence relative to WT (as %) from four to five separate experiments. Error bars indicate ± SEM; *$p < 0.05$ and ***$p < 0.001$ compared with ρ1WT.

expression, which was similar to ρ1WT (97.3% ± 5.4% of WT, $p > 0.05$).

Finally, complete deletion of the putative N-terminal α-helix as well as the N-terminal extension in the ρ1D61 construct eliminated detectable GABA-activated currents (data not shown). This correlated with an essentially complete loss of detectable ρ1D61 at the cell surface (3.5% ± 2.0% of ρ1WT, $p < 0.0001$). The total expression of ρ1D61 measured in permeabilized cells was similar to WT (96.4% ± 9.1% of ρ1WT) (Figure 5) indicating that the lack of detectable or functional ρ1D61 at the cell surface was due to a failure of receptor folding, assembly or trafficking.

To determine the role of the putative N-terminal α-helix independent of the N-terminal extension, we created a mutant that retained the N-terminal extension and replaced the putative α-helix with a shorter GTGSGTGS sequence (Figure 1C, defined as ρ1helix−coil), predicted to form a random coil able to span the same distance as the longer helix. This ρ1helix−coil mutant did give rise to GABA-activated currents, but the peak current was significantly decreased ($p < 0.0001$) to 8% ± 1% of ρ1WT (Table 1, Figure 3). Due to the small currents, it was not feasible to obtain a reliable measure of the GABA EC_{50} for the ρ1helix−coil mutant.

Immunofluorescent detection with the anti-ρ1 (N19) antibody, using flow cytometry (Figure 4C), showed that cell surface levels of the ρ1helix−coil mutant were only 10.3% ± 0.3% of ρ1WT ($p < 0.0001$), consistent with the reduced whole-cell peak current. Reduced cell-surface levels were not due to a decrease in total expression, however, since this was similar to ρ1WT (102% ± 7% of ρ1WT) (Figure 4C). We also examined receptor localization using confocal microscopy. HEK-293T cells expressing ρ1WT or ρ1helix−coil were stained

dx.doi.org/10.1021/cn500220t | ACS Chem. Neurosci. 2014, 5, 1266−1277

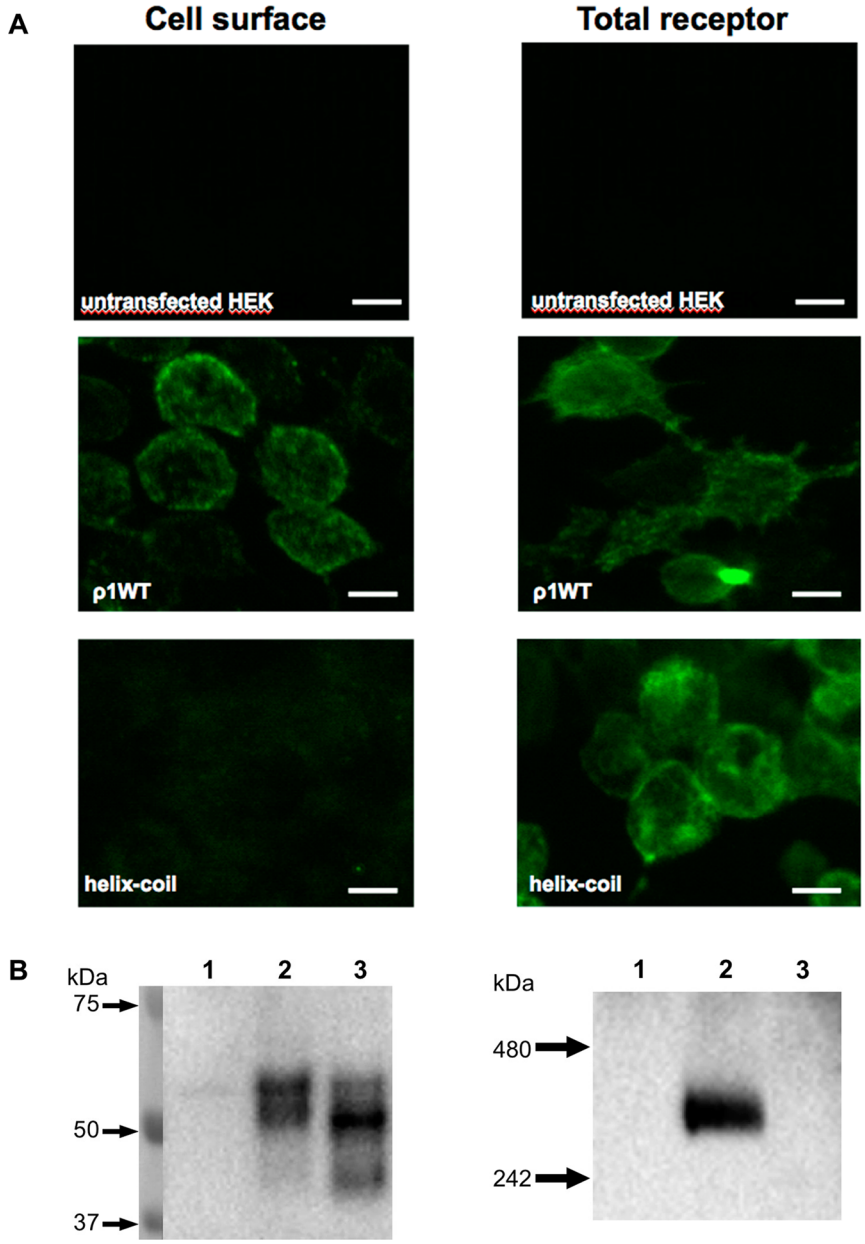

Figure 6. Anti-ρ1 (N19) immunodetection of ρ1WT and ρ1helix−coil. (A) Immunofluorescence images from confocal microscopy of (left) cell surface staining from nonpermeabilized HEK-293T cells or (right) total receptor staining from permeabilized cells that were either untransfected or transfected with ρ1WT and ρ1helix−coil mutant. White bars correspond to 10 μm. (B) Western blots with anti-ρ1 (N19) antibody of (left) reduced SDS-PAGE gel and (right) blue-native PAGE gel. In both cases lanes are (1) untransfected control, (2) ρ1WT, and (3) ρ1helix−coil mutant.

with anti-ρ1 (N19) antibody, followed by an Alexa Fluor 488 secondary antibody. Strong fluorescence was apparent for ρ1WT in both nonpermeabilized and permeabilized cells, but no cell surface or internal labeling was observed in untransfected cells (Figure 6A), demonstrating that labeling is specific to the presence of ρ1 $GABA_CRs$. Nonpermeabilized cells showed little or no detectable ρ1helix−coil at the cell surface, but permeabilized cells were strongly fluorescently stained, demonstrating robust intracellular levels of the ρ1helix−coil mutant. Thus, immunofluoroscence studies, using both flow cytometry and confocal microscopy, show that replacement of the putative α-helix in ρ1 $GABA_CR$ with a random-coil impairs the appearance of receptor protein at the cell surface, providing an explanation for the reduction in whole cell GABA-activated currents.

To determine whether the reduced trafficking of receptors to the cell surface is due to a defect in assembly of pentamers, samples of cells expressing ρ1WT and ρ1helix−coil were subjected to both SDS-PAGE and native gel electrophoresis, followed by Western blot detection using the anti-ρ1 (N19) antibody (Figure 6B). Reduced SDS-PAGE of ρ1WT showed a series of bands at just over 50 kDa molecular weight (MW), consistent with a predicted mature MW from sequence of 53.5 kDa and variable level of glycosylation at the three predicted extracellular N-glycosylation sites. The ρ1helix−coil mutant has only a 1.0 kDa lower predicted MW and showed a similar series of bands but in contrast to ρ1WT, the lowest MW band was strongest, indicating a lack of glycosylation. Because glycosylation is integral to the process of protein assembly and trafficking from the endoplasmic reticulum (ER) to the plasma

membrane, a lack of glycosylation is well recognized as a sign of ER-retention. A lower MW band of about 40 kDa was also apparent for the ρ1helix−coil mutant, indicating some partial degradation.

To investigate whether the reduced trafficking and glycosylation of the ρ1helix−coil was due to defective pentamer assembly, we turned to native-PAGE. Anti-ρ1 (N19) detected a single band at approximately 300−400 kDa for ρ1WT on blue native-PAGE (Figure 6B), consistent with an expected homopentamer. In contrast, no band was detected for the ρ1helix−coil mutant, indicative of a lack of assembled pentamers. Taken together, these data indicate that poor trafficking of ρ1helix−coil to the cell surface is due to a defect in pentamer assembly. The apparent stability of ρ1helix−coil in the ER by microscopy, FACS, and SDS-PAGE may suggest that, although not assembled into pentamers, individual subunits are relatively well folded and resistant to degradation.

DISCUSSION

LGIC function requires subunit folding, receptor assembly, trafficking to the cell surface, and intact ligand-gating channel mechanisms. A failure of any step in the process may lead to a loss of function. Furthermore, a measured deficit in later steps such as function or trafficking may be due to a failure in earlier steps. We have tested here the hypothesis that N-terminal regions of the ρ1 $GABA_C$R are not essential for ligand-gated ion channel function. This hypothesis arose from the identification and structure determination of bacterial pLGICs that lack these N-terminal regions yet form functional ligand-gated ion channels. The N-terminal region in question can be separated into two main segments. First, a putative α-helical region is consistently predicted just prior to the first highly conserved motifs in eukaryotic pLGICs. Although poorly conserved in sequence, an α-helix is structurally conserved at this position in all eukaryotic pLGIC structures determined to date but is absent from the two prokaryotic structures. Second, many eukaryotic pLGICs, although not nAChRs, have an "N-terminal extension" of variable length prior to the putative N-terminal α-helix. This extension is particularly long in the ρ1 $GABA_C$R.

Removal of both the N-terminal extension and putative α-helix in our ρ1D61 construct prevented the appearance of receptors at the cell surface and abolished GABA-activated whole cell currents. A lesser deletion in our ρ1T47 construct that retains the putative N-terminal α-helix but lacks the N-terminal extension showed robust levels of receptors at the cell surface and substantial GABA-gated ion channel function. The converse ρ1helix−coil mutant that retains the N-terminal extension but has the putative α-helix replaced with a random coil showed a marked reduction in both whole-cell peak currents and the number of receptors at the cell surface to approximately 10% of ρ1WT. These results combined demonstrate that the putative N-terminal α-helix is a critical region for trafficking of ρ1 $GABA_C$Rs to the cell surface. This result is consistent with two earlier reports demonstrating that removal of the putative N-terminal α-helix in α7 nAChRs also eliminated functional cell surface receptors.[30,31]

In contrast to complete deletion of the putative N-terminal α-helix, the ρ1E55 construct that retains half of the putative helix did produce functional channels at the cell surface. The whole cell currents and numbers of ρ1E55 receptors at the cell surface were, however, both significantly reduced to <30% of WT. Thus, six residues at the C-terminus of the putative helical region are able to partially restore receptor trafficking that is lost completely in ρ1D61. It is of note that this six-residue region overlaps α7 nAChR L11, which when mutated to alanine or proline essentially abolished receptor appearance at the cell surface.[30,31] The critical role for this residue is not completely conserved, since an equivalent mutation in the human α1 glycine receptor had no major effect on whole cell currents. Taken together, our results strengthen the evidence that the N-terminal α-helix, particularly the C-terminal half, is critical for trafficking of functional eukaryotic pLGICs to the cell surface. They also broaden this evidence to pLGICs other than α7 nAChRs.

Unlike nAChRs, other pLGICs have significant N-terminal extensions prior to the putative α-helix, including approximately 50 residues in the ρ1 $GABA_C$R. As shown in Figure 1A, an extension of this size could readily interact extensively with a neighboring subunit. Removal of this extension, in our ρ1T47 construct, did not prevent the appearance of functional receptors at the cell surface. It did, however, significantly reduce by >40% both the number of receptors at the cell surface and the maximum GABA-activated current amplitudes. We also found that deletion of roughly the middle third of the N-terminal extension, in a previously described splice variant, ρ1Δ51,[2] significantly reduced both cell-surface receptors and maximum currents by >20%. Because maximum whole-cell current amplitudes from transiently transfected channels are inherently highly variable, large numbers of measurements are required for sufficient power to relatively subtle changes such as this. The measurement of up to 20 cells in each IonFlux-16 ensemble whole-cell experiment markedly reduces current variability, however, and enhances statistical comparisons. Interestingly, a recent study showed that a β3 $GABA_A$R G32R mutation in the predicted N-terminal extension reduced whole-cell peak current and the amount of receptor at the cell surface,[35] providing further evidence of the importance of this region in receptor trafficking. As a whole, these results demonstrate that although the N-terminal extension is not required for functional receptors, it is an important determinant of how efficiently receptors are assembled and trafficked to the cell surface.

There is an overall trend in our data showing that with each N-terminal segment deleted, there is a stepwise decrease in the amount of functional receptor trafficked to the cell surface. This ends with a complete loss of receptors at the cell surface when the N-terminal extension and putative α-helix are deleted up to D61. Thus, each of the N-terminal segments we tested makes some contribution to receptor trafficking. Interestingly, none of our deletion mutants showed any reduction in total receptor expression, detected by flow cytometry of immunofluorescently labeled permeabilized cells. So, although not trafficked to the cell surface, ρ1 subunits with N-terminal deletions were not degraded, suggesting that these subunits were still properly folded. Nascent pLGIC subunits are translated into the ER where they are folded, assembled, and glycosylated prior to trafficking via the Golgi apparatus to the plasma membrane, whereas misfolded subunits are retrotranslocated from the ER for degradation by the proteasome.[36,37] We have shown that the ρ1helix−coil mutant that is poorly trafficked to the cell surface has a failure in pentamer assembly and is only weakly glycosylated, consistent with ER retention, but is relatively stable intracellularly. This is consistent with the work of Castillo et al., showing similar stable intracellular expression of α7 nAChRs with N-terminal α-helix mutations and demonstrating that for one of these mutants, L11P, subunits remained

monomeric rather than assembling into pentamers.[30] Although monomeric α1 or β2 $GABA_A$Rs subunits show some degradation,[38] these monomers or $\alpha1\gamma2$ or $\beta2\gamma2$ dimers, retained in the ER by interactions with immunoglobulin heavy-chain-binding protein (BiP) and calnexin,[39] are also relatively stable intracellularly despite not trafficking to the plasma membrane as functional receptors.[40] Thus, the importance of the N-terminal α-helix, and to a lesser extent the N-terminal extension, in receptor trafficking appears to be due to a role in assembly of subunits into pentameric receptors rather than in folding of each subunit.

Functional cell surface receptors lacking the N-terminal extension (ρ1T47) showed a dose−response for GABA-activated currents with a significantly smaller Hill coefficient. Although it is known that the agonist sensitivity of GlyRs is affected by receptor density, the reduced Hill coefficient of ρ1T47, described here, is not due to a decrease in receptor density at the cell surface. We found no correlation between whole cell current magnitude and either the GABA EC_{50} or Hill coefficient in ρ1WT or ρ1T47 (Supplementary Figures 1 and 2, Supporting Information). Because the Hill coefficient is a measure of the cooperativity of agonist binding between the multiple agonist sites in a receptor, this decrease is an indication of less concerted conformational changes between agonist sites. Given the location of the N-terminal extension at the subunit interface (Figure 1), its contribution to concerted conformational change may be due to participation in intersubunit interactions. The $\rho1\Delta51$ splice variant, with a lesser deletion within the same region, did not show a significant change in either GABA EC_{50} or Hill coefficient. Previous analysis of the $\rho1\Delta51$ splice variant in *Xenopus* oocytes showed an increased Hill coefficient and a lower EC_{50}, relative to WT, but no statistical significance was stated for these findings.[2] There are clear differences in the kinetics of ρ1 GABA responses when expressed in *Xenopus* oocytes versus HEK293T cells that may underlie this inconsistency in GABA EC_{50} and Hill coefficient changes.

The extracellular N-terminal domain has long been known as a major determinant of receptor assembly,[41−44] but our data and other recent findings[30,31] more specifically define an assembly role for the N-terminal region prior to the β-sandwich domain. Recent bacterial pLGIC structures have redefined the minimal core structure for this family, indicating that some segments in eukaryotic pLGICs may not be essential. The long intracellular M3−M4 loop in eukaryotic pLGICs, lacking in bacterial homologues, can be deleted without major functional consequence.[45] Conversely, we have shown here that the putative N-terminal α-helix, also lacking in bacterial pLGICs, is essential for the assembly and trafficking of functional ρ1 $GABA_C$R but not for the stability of intracellular subunits. Together with similar results for α7 nAChRs,[30,31] these results support the concept that, while not essential for subunit folding, N-terminal α-helices of eukaryotic pLGICs are critical for assembly of both cation- and anion-selective pLGICs. We showed further that additional residues prior to the putative N-terminal α-helix, particularly characteristic of anion-selective pLGICs, are not essential for functional ρ1 $GABA_C$Rs but do contribute to their assembly and trafficking and to the cooperativity of agonist activation. Although bacterial pLGICs assemble effectively without these two N-terminal regions, they do have other additional segments, a helical region between β-strands 3 and 4 in ELIC and an extended loop between β-strands 7 and 8 in GLIC, both of which contribute to intersubunit interactions and may facilitate pentamer assembly. Although built upon common core domains, eukaryotic and prokaryotic pLGICs appear to have evolved different intersubunit interactions that may differentially contribute to both pentamer assembly and allosteric mechanisms.

METHODS

Construction of ρ1 $GABA_C$R Mutants. The WT human ρ1 $GABA_C$R subunit cDNA was cloned into the mammalian expression vector pCDNA3.1. Deletion mutants of ρ1 were introduced using the QuickChange site-directed mutagenesis kit (Stratagene, La Jolla, CA) (ρ1T47) or by two-step mutagenesis followed by sequence and ligation independent cloning (SLIC)[46] into ρ1WT in pCDNA3.1 digested with *Nde*I and *Eco*RI ($\rho1\Delta51$, ρ1E55, and ρ1D61). Flanking primers in the PCR: fwd/*Nde*I 5′-CTGCCCACTTGGCAGTAC-ATC-3′ and rev/*Eco*RI 5′-TGCTGTAGAAAGCCAGTTTGG-3′ created homologous overlaps of approximately 30 bases to allow recombination with the cut vector. All constructs were verified by sequencing (Australian Genome Research Facility Ltd.). The first mature residue (T1) was retained in all these deletion constructs to ensure fidelity of signal peptide cleavage.

Cell Culture and Transfection. Human embryonic kidney (HEK-293T) cells were grown in Dulbecco's modified Eagle medium (DMEM) (Invitrogen, Life Technologies) supplemented with 10% fetal bovine serum (SAFC Biosciences) and antibiotic (penicillin/streptomycin) in a 37 °C incubator under a 5% CO_2 atmosphere. Cells were plated onto 6-well tissue culture-treated plates (Corning, NY) a day before transfection and grown to 80−90% confluency prior to transfection. WT or deletion constructs of ρ1 $GABA_C$R were transfected using Lipofectamine 2000 transfection reagent (Invitrogen, Life Technologies) according to the manufacturers' instructions. A total of 4 μg of plasmid DNA with 10 μL of Lipofectamine 2000 was used for each transfection. The cells were then incubated at 37 °C for 36−48 h prior to experiment.

Western Blotting. For sodium dodecyl sulfate polyacrylamide gel electrophoresis (SDS-PAGE), transiently transfected cells in 6-wells plates were harvested, washed with phosphate buffered saline (PBS), and resuspended in PBS. Approximately 50000 cells (per sample) were homogenized with a PRO2000 homogenizer (Bioworld, AUS), and then NuPAGE sample buffer (Invitrogen, Life Technologies) was added to 1× concentration with 50 mM DTT, and the mixture was heated at 80 °C for 10 min. Samples were loaded on NuPAGE 4−12% Bis-Tris gels (Invitrogen, Life Technologies) or nUView 4−20% Tris-glycine gels (NuSep), together with Precison Plus Protein Standards (Bio-Rad), and run at a constant voltage of 200 V for 45 min in 3-(*N*-morpholino)propanesulfonic acid (MOPS) SDS running buffer (Invitrogen, Life Technologies) or Tris-glycine buffer (NuSep), respectively, in an XCell SureLock mini-cell (Invitrogen, Life Technologies). Total protein loaded onto nUView gels was visualized after 2 min activation with UV light, to confirm approximately similar loading.

For native polyacrylamide gel electrophoresis (Native-PAGE), transiently transfected cells in 6-wells plate were harvested and washed with PBS. Approximately 50000 cells were prepared with NativePAGE sample buffer (Invitrogen, Life Technologies) and 2% digitonin in PBS and then incubated at 4 °C for 30 min. NativePAGE coomassie G-250 sample additive (Invitrogen, Life Technologies) was added to samples at 5%, immediately prior to electrophoresis on a NativePAGE 4−16% Bis-Tris gel (Invitrogen, Life Technologies), together with NativeMark unstained protein standards (Invitrogen, Life Technologies), at a constant voltage of 150 V for 120 min. After electrophoresis, proteins were transferred to poly(vinylidene fluoride) (PVDF; Bio-Rad) blotting membrane via electrophoretic Western transfer at 100 V for 1 h at 4 °C. Total high MW protein transferred to the membrane was visualized by staining with residual coomassie from electrophoresis, to confirm approximately similar loading. Membranes were then incubated with agitation at 4 °C; initially blocked overnight with 5% skim milk in Tris-buffered normal saline (TBS), followed by 1 h in 1/500 goat polyclonal anti-ρ1 $GABA_C$R primary antibody N19 sc-

7348 (Santa Cruz, Biotechnology) in TBS with 5% skim milk, three 15 min washes in TBS, 1 h in 1/2000 donkey anti-goat horseradish peroxidise-conjugated antibody (Santa Cruz, Biotechnology) in TBS with 5% skim milk, and finally three further 15 min washes in TBS. Labeling was detected with SuperSignal West Femto maximum sensitivity substrate (Thermo Scientific) for 5 min and visualized using a ChemicDocTM XRS+ (Bio-Rad) imaging system.

Flow Cytometry Analysis. For flow cytometric analysis of ρ1 expression, transiently transfected cells were harvested, resuspended in PBS, and washed twice with PBS on ice. Cells were kept on ice for all subsequent steps. For detection of total ρ1 expression, cells were fixed with 4% paraformaldehyde for 20 min, then permeabilized with 0.2% Triton X-100 (Sigma-Aldrich, USA) for 15 min and washed again with PBS. For detection of cell-surface ρ1 receptors, cells were not fixed or permeabilized prior to antibody staining. All cells were blocked with 10% horse serum (Gibco, Life Technologies) in PBS for 1 h, then incubated with a 1/200 dilution of goat polyclonal anti-ρ1 $GABA_CR$ antibody N19 sc-7348 (Santa Cruz, Biotechnology) or 1/500 dilution of mouse anti-His tag antibody (Invitrogen, Life Technologies) for 1 h. The cells were washed twice with PBS for 15 min each and incubated with 1/200 dilution of secondary donkey anti-goat antibody Alexafluor 488 (Invitrogen, Life Technologies) or goat anti-mouse antibody Alexafluor 633 (Invitrogen, Life Technologies) in the dark for 1 h and again washed twice in PBS for 15 min each. Cell-surface stained cells were then fixed with 4% paraformaldehyde for 20 min and washed with PBS for 15 min. The fluorescence intensity (FI) of 10000 cells from each sample was measured using a BD FACS Canto II (BD Biosciences) flow cytometer. Each experiment included negative control untransfected cells and positive control WT ρ1 transfected cells, stained in the same manner as mutant samples. The background mean FI of untransfected cells was subtracted from the mean FI of all other samples, and the resulting mean fluorescence of each mutant was expressed as a percentage of WT ρ1, within each experiment. These percentages were averaged across multiple experiments.

Electrophysiology. Electrophysiological measurement of ρ1 $GABA_CR$ currents were carried out with a 96-well plate automated electrophysiology platform (IonFlux-16 System) developed by Fluxion Biosciences, USA,[32,47,48] using ensemble plates to record total current from up to 20 cells. GABA was applied through microfluidic channels, integrated in the measurement plate, with a typical 10−90% solution exchange of approximately 50 ms across the population of cells (data not shown). Adherent transiently transfected cells were washed with PBS, then incubated with TrypLE (Invitrogen, Life Technologies) for 2−5 min. The cells were resuspended in serum free media (Invitrogen, Life Technologies), harvested by centrifugation at 1000 rpm for 2 min and washed three times with extracellular solution (in mM: 138 NaCl, 4 KCl, 1 $MgCl_2$, 1.8 $CaCl_2$, 10 4-(2-hydroxyethyl)-1-piperazineethanesulfonic acid (HEPES), 5.6 glucose, pH 7.45 with NaOH). Finally, cells were resuspended in extracellular solution at a concentration of 2−5 million cells/mL for electrophysiology. The intracellular solution was (in mM): 15 NaCl, 60 KCl, 70 KF, 5 EGTA, 5 HEPES, pH 7.25 with KOH. GABA was prepared as stock solution of 1 M in filtered water and stored at −20 °C. GABA dilutions were prepared on the day of the experiment by diluting the stock solution to desired concentration in extracellular solution. The cell membrane potential was clamped at a holding potential of −80 mV, and whole-cell currents were recorded. Each GABA application lasted for 3 s, with a 2 min wash between applications to allow the receptors to recover from desensitization. Recordings were performed at room temperature (22−25 °C).

Data Analysis and Statistics. Jpred3[49] (http://www.compbio.dundee.ac.uk/www-jpred/) was used for secondary structure predictions. Because secondary structure predictions are not precise, we allowed a generous definition of the putative N-terminal α-helix of the ρ1 $GABA_CR$ (T47−I60, Figure 1C), a region that encompasses all aligned helices in experimental structures (Figure 1B). Electrophysiology data were analyzed with integrated Fluxion software and Axograph X (http://www.axograph.com/). For each individual experiment, complete GABA dose response data were recorded and peak currents fitted to the Hill equation $I = I_{max}/(1 + 10^{(\log EC_{50} - \log X)n_H})$, where X is the agonist concentration, I is current, and n_H is the Hill coefficient. EC_{50} and Hill coefficients from these fits were averaged from four to seven experiments. For dose−response figures, each individual dose−response was normalized to the I_{max} from the individual fit to the Hill equation. Normalized data were then averaged and plotted, together with a fit of the Hill equation to the averaged data. Prism 6 (GraphPad Software Inc. La Jolla, CA) was used for curve fitting to data and statistical analysis. Data are presented as means ± SEM. The significance of differences was calculated using the Student's unpaired t test, with $p < 0.05$ considered indicative of a significant difference (GraphPad Prism Software).

■ ASSOCIATED CONTENT

Supporting Information

Figures showing a lack of correlation between current size and GABA dose−response parameters, EC_{50} and Hill coefficient. This material is available free of charge via the Internet at http://pubs.acs.org.

■ AUTHOR INFORMATION

Corresponding Author

*Brett A. Cromer. E-mail: brett.cromer@rmit.edu.au.

Author Contributions

Participated in research design: L.W.W., H.S.T., and B.A.C. Conducted experiments: L.W.W. Contributed reagents or analytic tools: B.A.C. Performed data analysis: L.W.W., H.S.T., and B.A.C. Wrote or contributed to the writing of the manuscript: L.W.W., H.S.T., and B.A.C.

Funding

This work was supported by a National Health and Medical Research Council (NHMRC) Project Grant (ID 566672). L.W.W. was supported by a University of Melbourne International Research Scholarship and Fee Remission Scholarship.

Notes

The authors declare no competing financial interest.

■ ABBREVIATIONS

EC_{50}, concentration required to elicit half-maximum response; $GABA_CR$, γ-aminobutyric acid type C receptor; pLGIC, pentameric ligand-gated ion channel

■ REFERENCES

(1) Thompson, A. J., Lester, H. A., and Lummis, S. C. R. (2010) The structural basis of function in Cys-loop receptors. *Q. Rev. Biophys. 43*, 449−499.

(2) Demuro, A., Martinez-Torres, A., and Miledi, R. (2000) Functional and pharmacological properties of GABArho1delta51 receptors. *Neurosci. Res. 36*, 141−146.

(3) Calvo, D. J., Vazquez, A. E., and Miledi, R. (1994) Cationic modulation of rho 1-type gamma-aminobutyrate receptors expressed in *Xenopus* oocytes. *Proc. Natl. Acad. Sci. U. S. A. 91*, 12725−12729.

(4) Cutting, G. R., Lu, L., O'Hara, B. F., Kasch, L. M., Montrose-Rafizadeh, C., Donovan, D. M., Shimada, S., Antonarakis, S. E., Guggino, W. B., Uhl, G. R., et al. (1991) Cloning of the gamma-aminobutyric acid (GABA) rho 1 cDNA: A GABA receptor subunit highly expressed in the retina. *Proc. Natl. Acad. Sci. U. S. A. 88*, 2673−2677.

(5) Wang, T. L., Guggino, W. B., and Cutting, G. R. (1994) A novel gamma-aminobutyric acid receptor subunit (rho 2) cloned from human retina forms bicuculline-insensitive homooligomeric receptors in Xenopus oocytes. *J. Neurosci. 14*, 6524−6531.

(6) Enz, R., and Cutting, G. R. (1999) GABAC receptor rho subunits are heterogeneously expressed in the human CNS and form homo-

and heterooligomers with distinct physical properties. *Eur. J. Neurosci. 11*, 41−50.
(7) Pan, Y., Ripps, H., and Qian, H. (2006) Random assembly of GABA rho1 and rho2 subunits in the formation of heteromeric GABA(C) receptors. *Cell. Mol. Neurobiol. 26*, 289−305.
(8) Ekema, G. M., Zheng, W., and Lu, L. (2002) Interaction of GABA receptor/channel rho(1) and gamma(2) subunit. *Invest. Ophthalmol. Vis. Sci. 43*, 2326−2333.
(9) Harvey, V. L., Duguid, I. C., Krasel, C., and Stephens, G. J. (2006) Evidence that GABA rho subunits contribute to functional ionotropic GABA receptors in mouse cerebellar Purkinje cells. *J. Physiol. 577*, 127−139.
(10) Milligan, C. J., Buckley, N. J., Garret, M., Deuchars, J., and Deuchars, S. A. (2004) Evidence for inhibition mediated by coassembly of GABAA and GABAC receptor subunits in native central neurons. *J. Neurosci. 24*, 7241−7250.
(11) Pan, Y., and Qian, H. (2005) Interactions between rho and gamma2 subunits of the GABA receptor. *J. Neurochem. 94*, 482−490.
(12) Qian, H., and Ripps, H. (1999) Response kinetics and pharmacological properties of heteromeric receptors formed by coassembly of GABA rho- and gamma 2-subunits. *Proc. Biol. Sci. 266*, 2419−2425.
(13) Reyes-Haro, D., Gonzalez-Gonzalez, M. A., Petriz, A., Rosas Arellano, A., Kettenmann, H., Miledi, R., and Martinez-Torres, A. (2013) Gamma-Aminobutyric acid-Rho expression in ependymal glial cells of the mouse cerebellum. *J. Neurosci. Res. 91*, 527−534.
(14) Brejc, K., van Dijk, W. J., Klaassen, R. V., Schuurmans, M., van Der Oost, J., Smit, A. B., and Sixma, T. K. (2001) Crystal structure of an ACh-binding protein reveals the ligand-binding domain of nicotinic receptors. *Nature 411*, 269−276.
(15) Miyazawa, A., Fujiyoshi, Y., and Unwin, N. (2003) Structure and gating mechanism of the acetylcholine receptor pore. *Nature 423*, 949−955.
(16) Unwin, N. (2005) Refined structure of the nicotinic acetylcholine receptor at 4A resolution. *J. Mol. Biol. 346*, 967−989.
(17) Prevost, M., Moraga Cid, G., Van Renterghem, C., Edelstein, S., Changeux, J.-P., and Corringer, P.-J. (2013) Intermediate closed state for glycine receptor function revealed by cysteine cross-linking. *Proc. Natl. Acad. Sci. U. S. A. 110*, 17113−17118.
(18) Cromer, B. A., Morton, C. J., and Parker, M. W. (2002) Anxiety over GABA(A) receptor structure relieved by AChBP. *Trends Biochem. Sci. 27*, 280−287.
(19) Ernst, M., Bruckner, S., Boresch, S., and Sieghart, W. (2005) Comparative models of GABAA receptor extracellular and transmembrane domains: important insights in pharmacology and function. *Mol. Pharmacol. 68*, 1291−1300.
(20) Mokrab, Y., Bavro, V. N., Mizuguchi, K., Todorov, N. P., Martin, I. L., Dunn, S. M. J., Chan, S. L., and Chau, P. L. (2007) Exploring ligand recognition and ion flow in comparative models of the human GABA type A receptor. *J. Mol. Graphics Modell. 26*, 760−774.
(21) Tasneem, A., Iyer, L. M., Jakobsson, E., and Aravind, L. (2005) Identification of the prokaryotic ligand-gated ion channels and their implications for the mechanisms and origins of animal Cys-loop ion channels. *Genome Biol. 6*, R4.
(22) Bocquet, N., Nury, H., Baaden, M., Le Poupon, C., Changeux, J.-P., Delarue, M., and Corringer, P.-J. (2009) X-ray structure of a pentameric ligand-gated ion channel in an apparently open conformation. *Nature 457*, 111−114.
(23) Hilf, R. J., and Dutzler, R. (2009) A prokaryotic perspective on pentameric ligand-gated ion channel structure. *Curr. Opin. Struct. Biol. 19*, 418−424.
(24) Hilf, R. J. C., and Dutzler, R. (2008) X-ray structure of a prokaryotic pentameric ligand-gated ion channel. *Nature 452*, 375−379.
(25) Hilf, R. J. C., and Dutzler, R. (2009) Structure of a potentially open state of a proton-activated pentameric ligand-gated ion channel. *Nature 457*, 115−118.
(26) Hibbs, R. E., and Gouaux, E. (2011) Principles of activation and permeation in an anion-selective Cys-loop receptor. *Nature 474*, 54−60.
(27) Miller, P. S., and Aricescu, A. R. (2014) Crystal structure of a human GABA receptor. *Nature 512*, 270−275.
(28) Hassaine, G., Deluz, C., Grasso, L., Wyss, R., Tol, M. B., Hovius, R., Graff, A., Stahlberg, H., Tomizaki, T., Desmyter, A., Moreau, C., Li, X.-D., Poitevin, F., Vogel, H., and Nury, H. (2014) X-ray structure of the mouse serotonin 5-HT3 receptor. *Nature 512*, 276−281.
(29) Zimmermann, I., and Dutzler, R. (2011) Ligand activation of the prokaryotic pentameric ligand-gated ion channel ELIC. *PLoS Biol. 9*, No. e1001101.
(30) Castillo, M., Mulet, J., Aldea, M., Gerber, S., Sala, S., Sala, F., and Criado, M. (2009) Role of the N-terminal alpha-helix in biogenesis of alpha7 nicotinic receptors. *J. Neurochem. 108*, 1399−1409.
(31) Bar-Lev, D. D., Degani-Katzav, N., Perelman, A., and Paas, Y. (2011) Molecular dissection of Cl-selective Cys-loop receptor points to components that are dispensable or essential for channel activity. *J. Biol. Chem. 286*, 43830−43841.
(32) Chen, Q., Yim, P., Yuan, N., Johnson, J., Cook, J., Smith, S., Ionescu Zanetti, C., Wang, Z.-J., Arnold, L., and Emala, C. (2012) Comparison of cell expression formats for the characterization of GABA(A) channels using a microfluidic patch clamp system. *Assay Drug Dev. Technol. 10*, 325−335.
(33) Yang, J., Cheng, Q., Takahashi, A., and Goubaeva, F. (2006) Kinetic properties of GABA rho1 homomeric receptors expressed in HEK293 cells. *Biophys. J. 91*, 2155−2162.
(34) Martinez-Torres, A., Vazquez, A. E., Panicker, M. M., and Miledi, R. (1998) Cloning and functional expression of alternative spliced variants of the rho1 gamma-aminobutyrate receptor. *Proc. Natl. Acad. Sci. U.S.A. 95*, 4019−4022.
(35) Gurba, K., Hernandez, C., Hu, N., and Macdonald, R. (2012) GABRB3 mutation, G32R, associated with childhood absence epilepsy alters $\alpha1\beta3\gamma2$L γ-aminobutyric acid type A (GABAA) receptor expression and channel gating. *J. Biol. Chem. 287*, 12083−12097.
(36) Kittler, J. T., McAinsh, K., and Moss, S. J. (2002) Mechanisms of GABAA receptor assembly and trafficking: implications for the modulation of inhibitory neurotransmission. *Mol. Neurobiol. 26*, 251−268.
(37) Vithlani, M., Terunuma, M., and Moss, S. (2011) The dynamic modulation of GABA(A) receptor trafficking and its role in regulating the plasticity of inhibitory synapses. *Physiol. Rev. 91*, 1009−1022.
(38) Gorrie, G. H., Vallis, Y., Stephenson, A., Whitfield, J., Browning, B., Smart, T. G., and Moss, S. J. (1997) Assembly of GABAA receptors composed of alpha1 and beta2 subunits in both cultured neurons and fibroblasts. *J. Neurosci. 17*, 6587−6596.
(39) Bollan, K., Robertson, L. A., Tang, H., and Connolly, C. N. (2003) Multiple assembly signals in gamma-aminobutyric acid (type A) receptor subunits combine to drive receptor construction and composition. *Biochem. Soc. Trans. 31*, 875−879.
(40) Sieghart, W. (1995) Structure and pharmacology of gamma-aminobutyric acidA receptor subtypes. *Pharmacol. Rev. 47*, 181−234.
(41) Hackam, A. S., Wang, T. L., Guggino, W. B., and Cutting, G. R. (1998) Sequences in the amino termini of GABA rho and GABA(A) subunits specify their selective interaction in vitro. *J. Neurochem. 70*, 40−46.
(42) Korpi, E. R., Kuner, T., Kristo, P., Kohler, M., Herb, A., Luddens, H., and Seeburg, P. H. (1994) Small N-terminal deletion by splicing in cerebellar alpha 6 subunit abolishes GABAA receptor function. *J. Neurochem. 63*, 1167−1170.
(43) Sumikawa, K. (1992) Sequences on the N-terminus of ACh receptor subunits regulate their assembly. *Mol. Brain Res. 13*, 349−353.
(44) Garcia-Guzman, M., Sala, F., Sala, S., Campos-Caro, A., and Criado, M. (1994) Role of two acetylcholine receptor subunit domains in homomer formation and intersubunit recognition, as revealed by alpha 3 and alpha 7 subunit chimeras. *Biochemistry 33*, 15198−15203.
(45) Jansen, M., Bali, M., and Akabas, M. H. (2008) Modular design of Cys-loop ligand-gated ion channels: functional 5-HT3 and GABA

rho1 receptors lacking the large cytoplasmic M3M4 loop. *J. Gen. Physiol. 131*, 137−146.
(46) Li, M. Z., and Elledge, S. J. (2007) Harnessing homologous recombination in vitro to generate recombinant DNA via SLIC. *Nat. Methods 4*, 251−256.
(47) Golden, A., Li, N., Chen, Q., Lee, T., Nevill, T., Cao, X., Johnson, J., Erdemli, G., Ionescu Zanetti, C., Urban, L., and Holmqvist, M. (2011) IonFlux: a microfluidic patch clamp system evaluated with human Ether-à-go-go related gene channel physiology and pharmacology. *Assay Drug Dev. Technol. 9*, 608−619.
(48) Spencer, C. I., Li, N., Chen, Q., Johnson, J., Nevill, T., Kammonen, J., and Ionescu Zanetti, C. (2012) Ion channel pharmacology under flow: automation via well-plate microfluidics. *Assay Drug Dev. Technol. 10*, 313−324.
(49) Cole, C., Barber, J. D., and Barton, G. J. (2008) The Jpred 3 secondary structure prediction server. *Nucleic Acids Res. 36*, W197−201.